Chirped Attosecond Photoelectron Spectroscopy

G. L. Yudin,[1,2] A. D. Bandrauk,[1] and P. B. Corkum[2]
[1]Laboratoire de Chimie Théorique, Université de Sherbrooke, Sherbrooke, Québec J1K 2R1, Canada
[2]National Research Council of Canada, Ottawa, Ontario K1A 0R6, Canada
(Received 7 October 2005; published 14 February 2006)

We study analytically the photoionization of a coherent superposition of electronic states and show that chirped pulses can measure attosecond time scale electron dynamics just as effectively as transform-limited attosecond pulses of the same bandwidth. The chirped pulse with a frequency-dependent phase creates the interfering photoelectron amplitudes that measure the electron dynamics. We show that at a given pump-probe time delay the differential asymmetry oscillates as a function of photoelectron energy. Our results suggest that the important parameter for attosecond science is not the pulse duration, but the bandwidth of phased radiation.

DOI: 10.1103/PhysRevLett.96.063002 PACS numbers: 32.80.Wr, 33.80.Wz

The development of femtosecond technology has been an interplay between the needs of science, demanding ever faster measurements, and technology producing ever shorter pulses [1]. Learning to compensate for dispersion, so that chirped pulses can be converted to transform-limited pulses and vice versa, has been one of the key advances [2]. Chirped pulses play an important role in technology [3], but transform-limited pulses are almost always used for measurement.

Attosecond technology is a radical departure from the ultrafast science that preceded it; see review [4]. Chirp is inherent in the attosecond generation process [5] except near the cutoff frequency [6]. Pulses with the broadest phased bandwidth will have substantial chirp [7], but the pulse duration and chirp can be measured [8,9] [see also [10] and references therein]. We address the question: "Are transform-limited pulses needed for rapid progress in attosecond science?"

To answer this question, we concentrate on single electron wave packets. Measuring electron dynamics in atoms and molecules [11–13] is a natural initial target for attosecond science. We show that, when measurement is via photoelectrons, chirped pulses allow the same time resolution limit as transform-limited pulses of the same bandwidth. What is essential is that the measurements are differential [14]. That is, the photoelectron spectrum is resolved in momentum and in space. Differential measurements are natural with large bandwidth attosecond pulses.

We assume that a pump pulse has prepared a coherent superposition of two bound states,

$$\Psi(\mathbf{r}, t) = \alpha_1 \Psi_1(\mathbf{r}, t) + \alpha_2 \exp(-i\beta)\Psi_2(\mathbf{r}, t), \quad (1)$$

where $\alpha_{1,2}^2$ are their populations ($\alpha_1^2 + \alpha_2^2 = 1$) and β is an adjustable initial phase that depends on the excitation scheme. The coherently prepared state is the simplest wave packet that can be formed. The pump pulse does not need to be short.

Now we consider single photon photoionization induced by a probe attosecond x-ray pulse. The probe pulse is precisely timed with respect to the phase of the pump pulse. Phasing occurs naturally in attosecond technology if the initial wave packet is excited by the fundamental pulse or its harmonics. We define the vector potential of such a pulse as a linearly chirped Gaussian

$$\mathbf{A}(t) = \mathbf{e}(A_0/2)\exp\left[-i\Omega t - \frac{(t - t_0)^2}{2\tau^2(1 - i\xi)}\right], \quad (2)$$

where Ω is the central frequency of the attosecond pulse, $\mathbf{e}$, A_0, and t_0 are the linear polarization vector, amplitude, and peak of the pulse. Positive dimensionless chirp ξ corresponds to the instantaneous frequency increasing with time. The pulse duration is $\tau_{\mathrm{FWHM}} = 2\tau\sqrt{\ln 2}\sqrt{1 + \xi^2}$.

The photoionization amplitude for the coherently coupled state (1) is given by

$$M_{\mathrm{coh}} = M_0\varepsilon[\gamma_1 M^{(1)} + \gamma_2 e^{-i\Phi(\xi, p, t_0)} M^{(2)}], \quad (3)$$

where $M_0 = A_0\tau[\pi(1 - i\xi)/2]^{1/2}$. $M^{(1)}$ and $M^{(2)}$ are the *monochromatic* photoionization amplitudes for the two bound states in the coherent superposition (1) for each photoelectron momentum. Attosecond photoelectron spectra depend on the x-ray pulse duration through the factors $\gamma_{1,2} = \alpha_{1,2}\exp(-\omega_{1,2}^2\tau^2/2)$, where $\omega_{1,2} = p^2/2 + I_p^{(1,2)} - \Omega$ (unless stated otherwise, we use atomic units $e = m_e = \hbar = 1$). $I_p^{(1,2)}$ are the ionization potentials of states $\Psi_1(\mathbf{r}, t)$ and $\Psi_2(\mathbf{r}, t)$. $\varepsilon = \exp(i\omega_1 t_0 + i\xi\omega_1^2\tau^2/2)$ is the phase factor in first attosecond ionization amplitude. The relative phase between amplitudes $\Phi(\xi, p, t_0)$ depends on β, t_0, photoelectron momentum, and chirp.

Equation (3) and Fig. 1 show that there are two contributions to the photoelectron spectrum. Dynamics is seen in the interference between the two contributions. Electron wave packet bandwidth does not depend on the linear chirp of the x-ray pulse [for example, the transform-limited $\tau_{\mathrm{FWHM}} = 24.19$ as (i.e., 1 a.u. of time) pulse and chirped pulse with $\tau_{\mathrm{FWHM}} = 250$ as and $\xi \approx 10$ generate electron wave packets with the same bandwidths]. For broad-bandwidth pulses photoelectron wave packets overlap

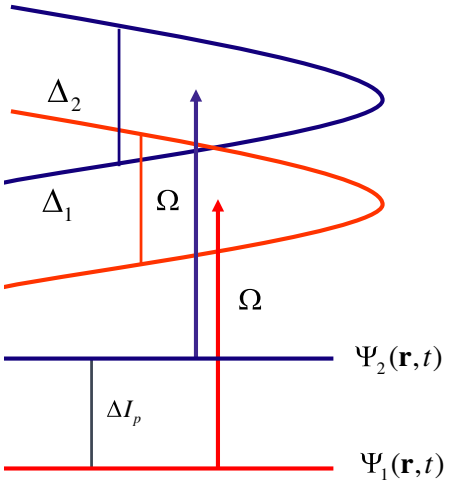

FIG. 1 (color online). A sketch of an electron wave packet generated by photoionization of a coherent superposition of electronic states. The bottom part of the figure represents the two bound states in the problem. The upper part plots the photoelectron momenta in the vertical direction and photoelectron probability in the horizontal direction originating from each bound state. Attosecond dynamics is measured in the overlap region.

and this spectral overlapping *is the same* for a given transform-limited pulse ($\xi = 0$) and its chirped equivalent.

Therefore, the resolution limit of a wave packet measurement is independent of the chirp. The interference, however, is different in details and we will show that this difference offers a new possibility for using chirped pulses to make single-time delay attosecond dynamics measurements.

The interference structure is determined by the full phase shift between amplitudes in Eq. (3),

$$\Phi(\xi, p, t) = \delta(t) + \phi(\xi, p). \tag{4}$$

This phase is universal and does not depend on the structure of the photoionization amplitudes $M^{(1)}$ and $M^{(2)}$. However, it depends on the chirp. The time-dependent phase shift $\delta(t) = \beta + \Delta I_p t$ parametrizes the bound electron motion. The chirp-dependent part of the full phase shift $\phi(\xi, p) = \xi\tau^2\Delta I_p[p^2/2 + I_p^{(\mathrm{av})} - \Omega]$ describes the chirped interference inside the photoelectron spectrum. $\Delta I_p = I_p^{(1)} - I_p^{(2)}$ is the level separation which depends on R in the molecular case and $I_p^{(\mathrm{av})} = (I_p^{(1)} + I_p^{(2)})/2$ is the average ionization potential of the coherently coupled electronic states.

Both phase factors are periodic. The factor $\exp[-i\delta(t_0)]$ which corresponds to electron "*hopping*" [12,15] is a periodic function of time with the period $T_0 = 2\pi/\Delta I_p$. The factor $\exp[-i\phi(\xi, p)]$ is a periodic function of the photoelectron energy $E_p = p^2/2$ with the period

$$E_0 = \frac{2\pi}{|\xi|\tau^2\Delta I_p} = \frac{T_0}{|\xi|\tau^2}. \tag{5}$$

So far, our description is completely general. However, for illustrative purposes it is useful to select a specific case. As theoretically tractable examples that capture the essence of our approach, we consider the hydrogen atom with a coherent superposition of $1s$ (atomic state $|1\rangle$) and $2s$ or $2p_0$ (atomic state $|2\rangle$) bound states or a H_2^+ molecular ion with a coherent superposition of two electronic states, $\sigma_g 1s$ (molecular state $|1\rangle$) and $\sigma_u 2p_0$ (molecular state $|2\rangle$). The electron and nuclear time scales in a molecule remain well separated so the nuclei are considered fixed. We assume that the molecule is aligned. At large internuclear distances we describe each molecular orbital as a linear combination of atomic orbitals. In our molecular model, the ion and electric field of the attosecond pulse are aligned along the z axis in Cartesian space.

We calculate the molecular photoionization amplitude using a final two-center Coulomb wave function. The molecular ionization transition amplitudes are determined by atomic amplitudes:

$$M_{\mathrm{mol}}^{(1,2)} \sim \chi M_{\mathrm{at}}^{(1,2)}, \tag{6}$$

where χ is the molecular interference factor [12,13]:

$$\chi = N_p[\exp(i\mathbf{pR}/2)G(-\mathbf{R}) + \exp(-i\mathbf{pR}/2)G(\mathbf{R})]. \tag{7}$$

$N_p = \exp(\pi/2p)\Gamma(1 + i/p)$ is the normalization factor, vector $\mathbf{R}$ is directed from one nucleus in a molecule to another, and $G(\mathbf{R})$ is the hypergeometric function, $G(\mathbf{R}) = F(i/p; 1; i(pR + \mathbf{pR}))$.

Using the dipole atomic monochromatic photoionization amplitudes M_{1s}, M_{2s}, and M_{2p_0} [see [13]], we will measure the angle and momentum resolved threefold photoelectron spectrum

$$\frac{d^3P_{\mathrm{coh}}(p, \theta, \varphi)}{dpd\Omega_e} \equiv S(p, \theta, \varphi) = p^2|M_{\mathrm{coh}}|^2, \tag{8}$$

where $d\Omega_e = \sin\theta d\theta d\varphi$ is the solid angle.

Figures 2 and 3 show the atomic photoelectron spectra $S(p, \theta, \varphi)$ for the case of $1s + 2s$ coherently coupled states. Because of the periodicity predicted by the phase shift (4), we present all results only in the interval $\delta \in [0, 2\pi]$. The populations of coherently coupled states are equal, ($\alpha_1^2 = \alpha_2^2$), the central photon energy $\Omega = 100$ eV, and the angle between polarization $\mathbf{e}$ and photoelectron momentum is $\theta = \pi/3$.

The spectra in Fig. 2 are generated by the so far shortest transform-limited $\tau_{\mathrm{FWHM}} = 250$ as pulse [6]. The time dependence of the whole spectrum is illustrated for two different dimensionless times δ. The momentum $p \approx 2.59$ corresponds to monochromatic photoionization from a level with the average ionization potential $I_p^{(\mathrm{av})}$. There we see the deviation between the two curves is large because the interference peaks here. In pump-probe spectroscopy dynamics is measured by delaying the probe pulse. The integrated signal changes with time. However, the changes originate in the interference region. The interference sig-

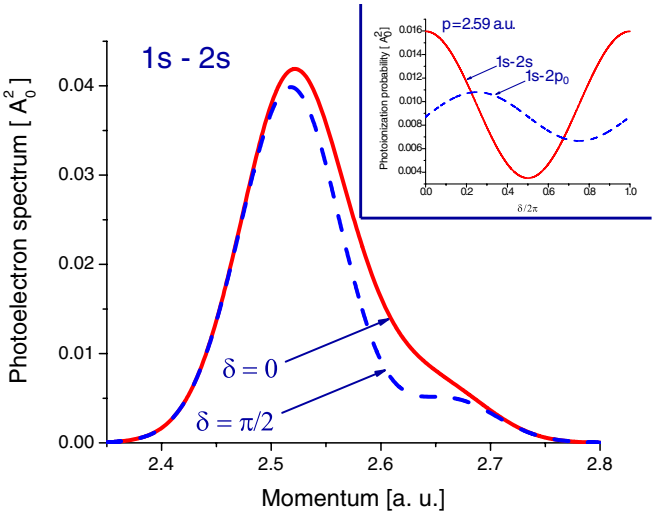

FIG. 2 (color online). The time-dependent atomic photoelectron spectra generated by the transform-limited $\tau_{\mathrm{FWHM}} = 250$ as pulse. The inset shows the interference signals as functions of time delay $\delta(t)$.

nals are plotted in the inset as functions of time delay for $1s + 2s$ and $1s + 2p_0$ couplings. As expected, we measure the 2π time periods (in scaled units). Note that in the case of $1s + 2p_0$ coherent atomic superposition, the interference is weaker in the high x-ray energy region because the transition amplitude M_{2p_0} is much less then the amplitude M_{2s}.

Interference will be present for all chirps at all time delays. Figure 3 shows that the dynamics can be determined from the interference spectrum itself. For this calculation we use a slightly broader bandwidth pulse. The spectra in Fig. 3 are generated by the transform-limited and chirped $\tau_{\mathrm{FWHM}} = 150\sqrt{1 + \xi^2}$ as pulses. Prominent in the

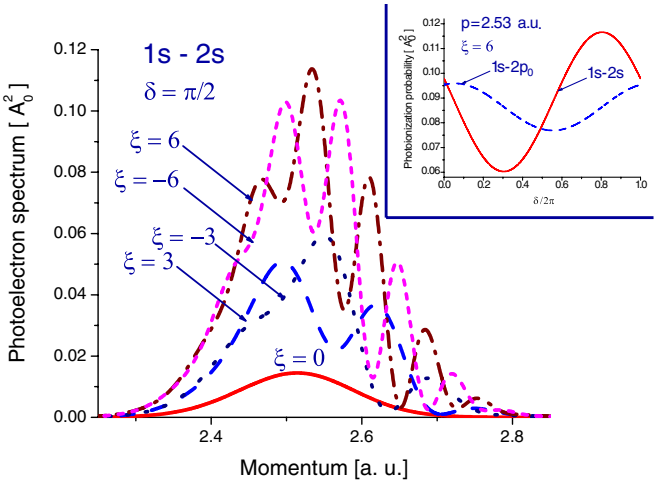

FIG. 3 (color online). The time- and chirp-dependent atomic photoelectron spectra generated by the transform-limited and chirped pulses. The inset shows the interference signals as functions of time delay $\delta(t)$.

figure is a modulation of the photoelectron spectrum. The modulation frequency is greater for larger chirp. It disappears for $\xi = 0$. Changing the sign of the chirp interchanges maxima and minima. The inset in Fig. 3 shows that pump-probe experiments can resolve the 400 as dynamics of the wave packets even for a pulse that is approximately 6×150 as $= 900$ as long. In fact, the modulation itself can be used to determine the attosecond wave packet dynamics. The energy difference between neighboring maxima or minima is approximately $E_0 \approx p\Delta p$, where p is the position of one maximum (minimum) and Δp is the difference in positions of neighboring maxima (minima). Substituting E_0 into Eq. (5) we determine time period T_0. Strictly speaking, the photoelectron spectra are not exactly periodic because $\gamma_{1,2}M^{(1,2)}$ in the coherent amplitude (3) are momentum dependent. The better the inequality $\Delta p \ll 1$ is satisfied, the more accurate is the periodicity.

Experimentally it may be more useful to measure the momentum asymmetry than the momentum spectrum because the momentum asymmetry is self-calibrating. The integral photoionization asymmetry [16] has already been used to measure the carrier envelope phase of intense few-cycle laser pulses [17]. In analogy with the integral asymmetry, we define the absolute (Δ) and normalized (Δ_N) differential asymmetries as

$$\Delta(p, \theta, \varphi) = S(p, \theta, \varphi) - S(p, \pi - \theta, \varphi), \tag{9}$$

$$\Delta_N(p, \theta, \varphi) = \frac{S(p, \theta, \varphi) - S(p, \pi - \theta, \varphi)}{S(p, \theta, \varphi) + S(p, \pi - \theta, \varphi)}. \tag{10}$$

In the molecular case, the asymmetry (9) is independent of the azimuthal angle φ since the molecule is aligned along the z axis. From Eqs. (3) and (9) we obtain the absolute atomic and molecular differential asymmetries:

$$\Delta_{\mathrm{at}}(p, \theta) = 2\pi(A_0\tau)^2\sqrt{1 + \xi^2}\alpha_1\alpha_2 p^2 \times \mathrm{Re}\{e^{-i\Phi(\xi,p,t_0)-(\omega_1^2+\omega_2^2)\tau^2/2}M_{1s}^* M_{2p_0}\}, \tag{11}$$

$$\Delta_{\mathrm{mol}}(p, \theta) \sim |\chi|^2\Delta_{\mathrm{at}}(p, \theta). \tag{12}$$

In the case of high x-ray frequencies, where $p \gg 1$, one obtains

$$\Delta_{\mathrm{at}}(p, \theta) \sim -\sin[\Phi(\xi, p, t_0)]\cos\theta(2\cos^2\theta - 1), \tag{13}$$

reflecting the time dependence and chirped interference (via the factor $\sin[\Phi(\xi, p, t_0)]$), $1s$ (via the factor $\cos\theta$), and $2p_0$ [via the factor $(2\cos^2\theta - 1)$] of interfering photoionization amplitudes.

Figures 4 and 5 show atomic and molecular differential asymmetries. In Fig. 4 we give the results for the time dependence (via the phase δ) of the atomic normalized asymmetry. Using the same parameters as in Fig. 3, we find that at some momenta all electrons go in one direction. The figure also shows how the modulation of the photoelectron spectrum moves as the pump-probe time delay changes.

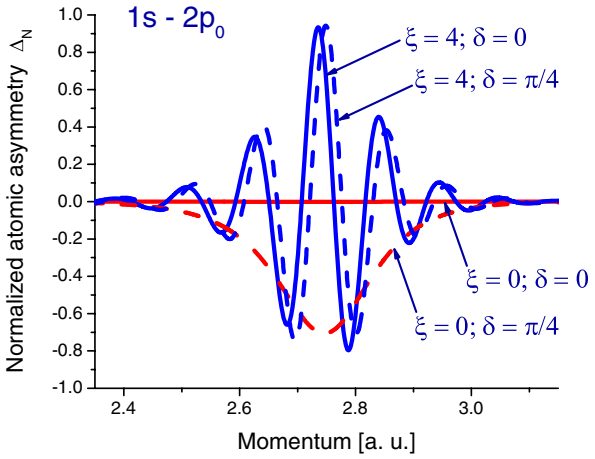

FIG. 4 (color online). The normalized time- and chirp-dependent atomic photoelectron differential asymmetries in photoelectron spectra generated by the transform-limited and chirped pulses.

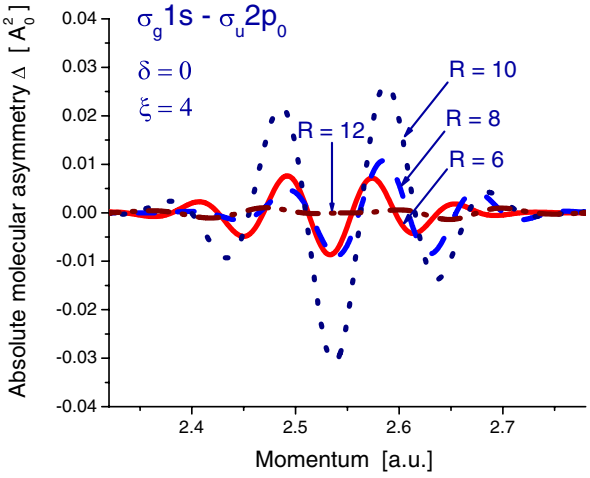

FIG. 5 (color online). Molecular interference in the absolute photoelectron differential asymmetry at chirp $\xi = 4$ and different internuclear distances R.

However, the modulation period remains the same. Note that, from the normalized atomic differential asymmetries we can extend the effective range of photoelectron momenta. In Fig. 4 this range extends from 2.4 to 3.05 a.u. while in the corresponding calculations for absolute differential asymmetries the range is from 2.4 to 2.75 a.u.

So far, we have shown how chirped pulses can be used to observe atomic wave packet motion. A diatomic molecule introduces a two-center interference. The absolute molecular asymmetries are displayed in Fig. 5 at large different internuclear distances. Changing the internuclear distance R the level separation, ΔI_p, slightly changes, but the interference pattern is defined mostly by the values of pR and $\mathbf{pR}$ in the interference factor (7). The photoelectron signal and, therefore, the absolute asymmetry at $R = 12$ is suppressed due to destructive molecular interference. The minimum value of $|\chi|^2$ in Fig. 5 is in the range of the photoelectron momenta.

In conclusion, we show that long chirped attosecond pulses can measure attosecond time scale electron dynamics. The dynamics can be measured just as effectively as if the pulses were transform limited. Pump-probe time delay spectroscopy is possible, but not necessary if chirped pulses are used. We also show that the oscillations in the photoelectron spectra are described by a universal phase shift between the interfering photoionization amplitudes. The phase shift allows us to read the dynamics at a single-time delay. We find that the differential normalized asymmetry of the photoelectrons can reach 100%. All electrons in some momentum windows are ionized in a given direction. The direction changes with time delay. This shows photoionization control with attosecond pulses.

Until now, the figure of merit of attosecond pulses has been the pulse duration. Our results imply that the emphasis of attosecond technology should shift from producing transform-limited pulses to producing broad-bandwidth pulses [18]. The pulses can be chirped or unchirped. All that is needed is that the chirp is well characterized.

We are grateful to S. Chelkowski and M. Yu. Ivanov for valuable discussions.

[1] J.-C. Diels and W. Rudolph, *Ultrashort Laser Pulse Phenomenon: Fundamentals, Techniques and Applications on a Femtosecond Time Scale* (Academic, New York, 1996).
[2] O. E. Martinez, IEEE J. Quantum Electron. **23**, 1385 (1987).
[3] D. Strickland and G. Mourou, Opt. Commun. **56**, 219 (1985).
[4] J. Levesque and P. B. Corkum, Can. J. Phys. **84**, 1 (2006).
[5] P. B. Corkum, Phys. Rev. Lett. **71**, 1994 (1993).
[6] R. Kienberger *et al.*, Nature (London) **427**, 817 (2004).
[7] Y. Mairesse *et al.*, Science **302**, 1540 (2003).
[8] J. Itatani *et al.*, Phys. Rev. Lett. **88**, 173903 (2002); Laser Phys. **14**, 344 (2004).
[9] Y. Mairesse and F. Quéré, Phys. Rev. A **71**, 011401(R) (2005); F. Quéré, Y. Mairesse, and J. Itatani, J. Mod. Opt. **52**, 339 (2005).
[10] P. Agostini and L. F. DiMauro, Rep. Prog. Phys. **67**, 813 (2004).
[11] H. Niikura, D. M. Villeneuve, and P. B. Corkum, Phys. Rev. Lett. **94**, 083003 (2005); H. Niikura *et al.*, J. Mod. Opt. **52**, 453 (2005).
[12] G. L. Yudin *et al.*, Phys. Rev. A **72**, 051401(R) (2005).
[13] G. L. Yudin, S. Chelkowski, and A. D. Bandrauk, J. Phys. B **39**, L17 (2006).
[14] A. Stolow, Annu. Rev. Phys. Chem. **54**, 89 (2003).
[15] A. D. Bandrauk, S. Chelkowski, and H. S. Nguyen, Int. J. Quantum Chem. **100**, 834 (2004).
[16] A. D. Bandrauk, S. Chelkowski, and N. H. Shon, Phys. Rev. Lett. **89**, 283903 (2002); Phys. Rev. A **68**, 041802(R) (2003).
[17] E. Goulielmakis *et al.*, Science **305**, 1267 (2004).
[18] R. K. Shelton *et al.*, Science **293**, 1286 (2001).